Solid-state structure, dynamical properties in solution and computational studies of a new sodium hemispherand complex

Frank C. J. M. van Veggel,†,[a] John P. M. van Duynhoven,[b] Sybolt Harkema,[c] Manon P. Oude Wolbers[d] and David N. Reinhoudt*,[d]

[a] *Akzo Research Laboratories Arnhem, PO Box 9300, 6800 SB Arnhem, The Netherlands*
[b] *Laboratories of Chemical Analysis, Faculty of Chemical Technology, University of Twente, PO Box 217, 7500 AE Enschede, The Netherlands*
[c] *Laboratories of Chemical Physics, Faculty of Chemical Technology, University of Twente, PO Box 217, 7500 AE Enschede, The Netherlands*
[d] *Laboratories of Organic Chemistry, Faculty of Chemical Technology, University of Twente, PO Box 217, 7500 AE Enschede, The Netherlands*

The solid-state structure of 1·$NaClO_4$ has been determined by X-ray diffraction and shows the Na^+ complexed in an approximate hexagonal bipyrimidal fashion. The six ether oxygens form the ground plane, the inner carbonyl group and one of the two outer carbonyl groups occupy the apical positions. The solution structure in methanol, as determined by NMR spectroscopy, has a time-averaged plane of symmetry through the inner phenyl ring. This plane of symmetry is the result of a fast interconversion of conformations in which either one of the outer carbonyl groups is coordinated to the Na^+. The enthalpy of activation in methanol determined by $T_{1\rho}$ measurements is 5 ± 1 kcal mol^{-1}. This process of fast exchange was supported by TRAVEL/CHARMm simulations which revealed a transition-state structure with the two outer carbonyl groups coordinated to the Na^+ with a plane of symmetry through the inner phenyl ring. The calculated activation energy is 6.1 kcal mol^{-1}, in very good agreement with the experimental value. A significant influence of the solvent on the structure of 1·Na^+ could be ruled out by an MD simulation in methanol. The structure is very similar to the solid-state structure.

For some years we have been searching for cation selective receptors that can be applied in membrane transport[1] and in sensors based on the chemically modified field effect transistor (CHEMFET).[2] The calix[4]arene platform[3] derivatized with four $CH_2C(O)NRR$ groups in the cone conformation provides a large Na^+ over K^+ selectivity.[4] For potassium a selective receptor has been synthesized based on a hemispherand.[5] Although since the introduction by Cram, a large number of pre-organized spherands and hemispherands[6] have been published, molecule **1**, with pendant substituents on the phenolic oxygens, has not been explored so far. From preliminary FABMS studies[7] we obtained indications that hemispherand **1** has a larger Na^+ over K^+ selectivity than the well known hemispherand **2**. After mixing ligand **2** with 1 equiv. of $NaClO_4$ and $KClO_4$ in MeOH the FABMS measurement in nitrobenzyl alcohol (NBA) gave a ratio **2**·Na^+:**2**·K^+ of 1:3, whereas ligand **1** gave a ratio of 150:1.

In this paper we report the synthesis, the solid-state structure, the solution structure and the dynamical properties of 1·Na^+. The structures and dynamics in the different phases are not necessarily the same and one has to be very cautious when extrapolating from one phase to the other. Dang and Kollman[8] have shown this for an MD simulation of the K^+ complex of 18-crown-6 in water. The starting structure was the solid-state structure in which the K^+ is fully encapsulated by the crown ether. During the simulation a rearrangement occurred to a structure that can be described as a sandwich. One face of the K^+ is occupied by the crown ether and the other by three molecules of water. Thus, the solvent has 'loosened' the K^+ from the crown ether. A similar observation was recently reported by Thompson *et al.*[9] in a hybrid quantum mechanical–molecular mechanics study. Experimental differences between the solid-state structure and structure in solution have been observed for the natural potassium ionophore, valinomycin. In solution the complex is present as a mixture of three conformations, the relative abundancies of which depend on the polarity of the solvent.[10] In the solid state the structure has an oval shape with six intramolecular hydrogen bonds and differs from the three conformers in solution.[11] A striking example from our own laboratories is the structure of the potassium complex of a calixspherand. The calix[4]arene skeleton is a partial cone and the terphenyl moiety can adapt two conformations with respect to the rotated phenyl ring of the calix[4]arene. In the solid state the terphenyl moiety has a conformation opposite to that in solution.[12]

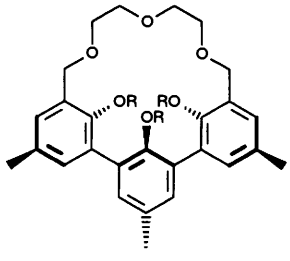

1 R = CH_2COOEt
2 R = Me

Results and discussion

Synthesis

The synthesis of 1·$NaClO_4$ was accomplished in three steps from the dibromide **3**.[13] The macrocyclic hemispherand

† Present address: Laboratories of Organic Chemistry, Faculty of Chemical Technology, PO Box 217, 7500 AE Enschede, The Netherlands.

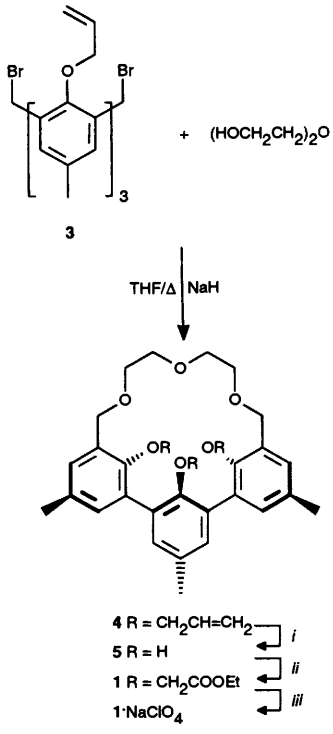

i HCOOH, Et_3N, $Pd(PPh_3)_4$, EtOH, H_2O,Δ.
ii $BrCH_2COOEt$, K_2CO_3, CH_3CN,Δ.
iii $NaClO_4$, MeOH.

4·$NaClO_4$ was prepared by the reaction of **3** with diethylene glycol, with NaH as a base in THF under high dilution conditions. The hemispherand was isolated as the $NaClO_4$ complex in 64% yield. The ^1H NMR spectrum of compound **4**·$NaClO_4$ shows the expected AB-quartet for the benzylic protons at δ 4.92 and 4.00 (J = 9.0 Hz). The macrocyclic nature of the product is also evident from the two doublets at δ 7.10 and 7.04 (J = 2.0 Hz) for the outer phenyl rings and the singlet at δ 7.30 for the inner phenyl ring. The FAB mass spectrum shows the highest m/z peak at 593, which corresponds to $(M + Na)^+$. The phenol groups in **4**·$NaClO_4$ could be deprotected by the palladium catalysed reaction described by Yamada *et al.*[14] The ^1H NMR spectrum shows the typical pattern for the terphenyl unit in a hemispherand indicating that the benzylic ethers are unaffected. The pendant arms in **1**·$NaClO_4$ were introduced by reaction of **5** with ethyl bromoacetate in refluxing acetonitrile with K_2CO_3 as a base. The new hemispherand **1** was isolated as the $NaClO_4$ complex in 63% yield. The FAB mass spectrum shows the highest m/z peak at 371, which can be attributed to $(M + Na)^+$. The ^1H NMR spectrum shows the expected AB-quartet for the benzylic protons at δ 5.01 and 4.20 (J = 10.0 Hz) and the two doublets at δ 7.25 and 7.18 (J = 2.0 Hz) and the singlet at δ 7.47 for the terphenyl moiety. The outer $ArOCH_2$ groups are observed as an AB-quartet at δ 4.22 and 4.04 (J = 16.0 Hz), whereas the inner $ArOCH_2$ is shifted upfield (singlet, δ 3.10). Owing to the fact that **1**·$NaClO_4$ has a plane of symmetry through the inner phenyl ring, the outer ethyl groups of the esters are observed as an ABX_3-system (δ 4.25–4.07).

Solid-state structure

Single crystals of **1**·$NaClO_4$ were grown by slow evaporation of a methanol solution. The structure is shown in Fig. 1. The Na^+ is completely encapsulated by the ligand in an approximate hexagonal bipyrimidal fashion. The inner carbonyl oxygen and only one of the outer carbonyl oxygens occupy the apical positions. The other outer substituent is not involved in coordination. The coordination distances of the ether oxygens

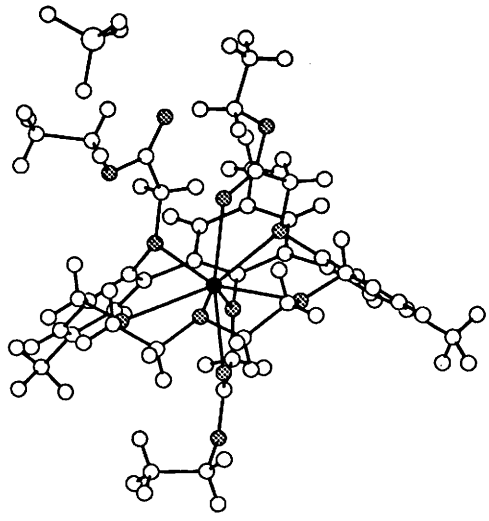

Fig. 1 X-Ray structure of **1**·$NaClO_4$

in **1**·Na^+ and **2**·Na^+[15] are very similar (Table 1), because the framework of the hemispherands is pre-organized. However, in **2** the sodium ion is somewhat less deeply buried in the hemispherand cavity. The angles between the phenyl rings are larger in **1**·$NaClO_4$ than in **2**·NaPic (Pic is picrate), which may be the result of crystal packing forces. The coordination distances of the two carbonyl oxygens are smaller than those of the ether oxygens because the carbonyl oxygen has a larger negative charge in combination with the flexibility of the pendant arms.

NMR studies

The ^1H and ^{13}C NMR spectra of **1**·$NaClO_4$ in CD_3OD solution show that on the chemical shift timescale, the complex has a plane of symmetry through the inner phenyl ring. The ^{13}C NMR spectrum is shown in Fig. 2. The two outer and the single inner phenyl rings are clearly reflected in the various sets of signals. All ^1H and ^{13}C NMR resonances were assigned in a straightforward manner by HMQC[16], DQ-[17] and TQ-COSY[18] experiments (see the Experimental section). The time-averaged structure of the complex in solution can be rationalized either because both outer carbonyl oxygens are coordinated to the Na^+ or by a fast interconversion of conformations in which either of the two outer carbonyl groups is coordinated to the Na^+. Variable temperature ^1H NMR spectra between 183 and 323 K show only a minor degree of line-broadening. This observation does not allow a choice between the two possibilities. However, rotating frame spin-lattice relaxation time ($T_{1\rho}$) measurements provide the opportunity to assess activation barriers of processes that are fast on the chemical shift timescale. When the molecule is in the fast tumbling regime ($\omega\tau_c \ll 1$) the exchange contribution to $T_{1\rho}$ can be evaluated from $T_{1\rho}$ and T_1 from eqn. (1).[19]

$$\frac{1}{T_{1\rho}^{ex}} = \frac{1}{T_{1\rho}} - \frac{1}{T_1} \quad (1)$$

From theoretical calculations of τ_c one can estimate that for **1**·Na^+ in methanol the fast tumbling regime applies for temperatures higher than *ca.* 260 K. Indeed, the ^1H T_1 values increase when the temperature is raised above this temperature and also the ^1H–^1H NOE's become positive (Fig. 3). For a dynamic interconversion of two sites with rate constant τ_e^{-1} with a chemical shift difference $\Delta\omega$ and for a given radiofrequent field ω_1, eqn. (2) can be derived.

$$T_{1\rho}^{ex} = \frac{4}{\Delta\omega^2\tau_{ex}} + \frac{4\omega_1^2\tau_{ex}}{\Delta\omega^2} \quad (2)$$

Table 1 Structural details of **1**·Na^+ in the solid state and computational studies. Some data of the solid-state structure of **2**·Na^+ are given for comparison.[15] Distances in Å and angles in degrees

	1·$NaClO_4$			
	X-Ray	Minimized structure	Saddle point	**2**·NaPicrate[a]
$ArO \cdots Na^+$	2.46–2.54	2.48–2.62	2.52–2.87	2.51–2.57
$ArCH_2O \cdots Na^+$	2.61/2.64	2.45/2.63	2.56/2.57	2.62/2.85
$O_{ether} \cdots Na^+$	2.34	2.31	2.32	2.46
$C{=}O_{inner} \cdots Na^+$	2.39	2.27	2.32	—
$C{=}O_{outer} \cdots Na^+$	2.54/4.74	2.29/4.70	2.39/2.40	—
Angle phenyl rings	−66.9/63.8	−54.9/62.0	−49.9/50.4	−56.5/53.6

[a] The picrate counter anion is bidentate coordinated; $PhO \cdots Na^+$ = 2.36 Å and $O_{nitro} \cdots Na^+$ = 2.62 Å.

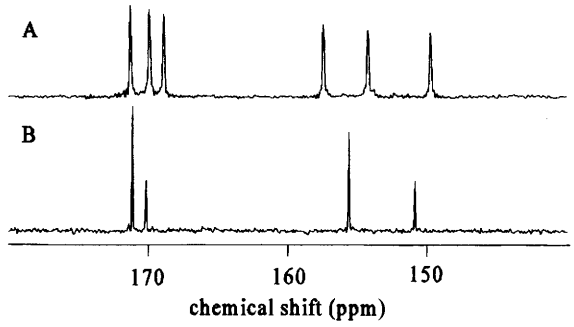

Fig. 2 ^{13}C NMR spectra of **1**·$NaClO_4$; (*a*) solid state (CPMAS) and (*b*) in CD_3OD solution

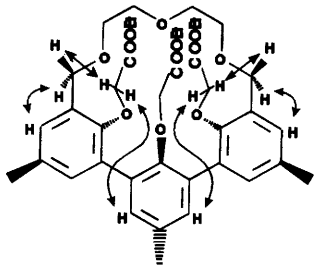

Fig. 3 Structure of **1**·$NaClO_4$ with some non-trivial NOEs

In the temperature range 223–323 K for most isolated ^1H NMR resonances the exchange contribution to $T_{1\rho}$ is very small, except for the axial benzylic resonances at 5.01 ppm. This can be attributed to the dynamics of the two outer carbonyl groups. In the range of ω_1 = 2–8 kHz, the $T_{1\rho}^{ex}$ value is independent of the strength of the applied radiofrequent field, hence $\omega_1\tau_{ex} \ll 1$. The activation enthalpy for the exchange process of the two outer carbonyl groups of 5 ± 1 kcal mol^{-1}‡ was determined from a plot of $T_{1\rho}^{ex}$ *vs.* T^{-1}. This result shows a fast interconversion of the two outer carbonyl oxygens in the coordination shell of Na^+, whereas the inner carbonyl oxygen remains coordinated to the Na^+. The solid-state (CPMAS) spectrum of **1**·$NaClO_4$ (Fig. 2) clearly shows that the complex does not possess a plane of symmetry because of the three resonances of the carbonyl carbons. The fact that the ^{13}C NMR resonances are not very different from those in CD_3OD solution shows that the overall structures are very similar.

Computational studies

In order to investigate the fast exchange process some computational studies were carried out. The coordinates of the X-ray structure were used as input in the energy minimization *in vacuo* with the CHARMM force field[20] [see Fig. 4(*a*)]. Comparison of the coordination distances with the solid-state structure shows that virtually no conformational change had occurred (Table 1). Only one angle between the phenyl ring changed considerably. This is exactly what can be expected for such a pre-organized ligand. Recently an algorithm, called Conjugate Peak Refinement, was published which allows the calculation of true saddle points on an adiabatic potential energy surface.[21] The algorithm is implemented as the TRAVEL module in CHARMm. The only input required are two local minima and the program will (iteratively) calculate a pathway with one or more saddle points connecting these two minima. We have applied this algorithm successfully for the calculations of the barriers of activation of the interconversions of calix[4]arenes.[22] The calculated values are within 1 kcal mol^{-1} of the experimental values. We have also predicted correctly the rotational barriers of guests imprisoned in a new type of carceplexes.[23]

A mirror image of the minimized structure of **1**·Na^+ was generated and the two local minima could be connected *via* a pathway with one saddle point (Fig. 5). The structure of the saddle point is given in Fig. 4(*b*). The two outer carbonyl oxygens are both coordinated to the Na^+ and apart from the ethyl groups of the outer ester groups there is a plane of symmetry through the inner phenyl ring.

The coordination distances and angles between the phenyl rings are summarized in Table 1. They show that the macrocyclic ring does not rearrange to a large extent. The energy barrier ΔE for this exchange process is 6.1 kcal mol^{-1}. The major contributions to the activation energy are: E_{angle} = 0.6, E_{dihe} = 3.6, E_{vdW} = −1.6 and E_{el} = 3.5 kcal mol^{-1}. These contributions show that coordination of the two outer carbonyl oxygens is less favourable than of one, largely owing to unfavourable dihedral and electrostatic energies. The TRAVEL calculations point to a fast exchange process but solvent effects, if any, have not been included. In order to include solvent effects, a molecular dynamics run (50 ps) was carried out in OPLS MeOH.[24] A structure with the two outer carbonyl groups coordinated was dissolved in a cubic box of MeOH with dimensions of 30.7 Å. During the heating and equilibration phase, NOE constraints were applied to the outer carbonyl oxygen $\cdots Na^+$ distances, which were released in the production phase.§ At the end of the equilibration phase the plane of symmetry was already (partly) lost ($C{=}O_{outer} \cdots Na^+$, 2.23 and 4.17 Å); it is apparently more favourable to have one $C{=}O_{outer}$ in the first coordination shell. The other $C{=}O_{outer}$ is initially weakly interacting with the Na^+, but within *ca.* 20 ps it points towards the solvent. The resulting overall structure resembles that of the solid state. The non-coordinated carbonyl oxygen is frequently involved in hydrogen bonding to the solvent. This MD simulation rules out any stabilization by methanol of a structure in which both outer carbonyl groups are coordinated to the Na^+. Our data are consistent with a fast

‡ 1 cal = 4.184 J.

§ The plane of symmetry was already lost during the (preliminary) minimization and heating phase without constraints.

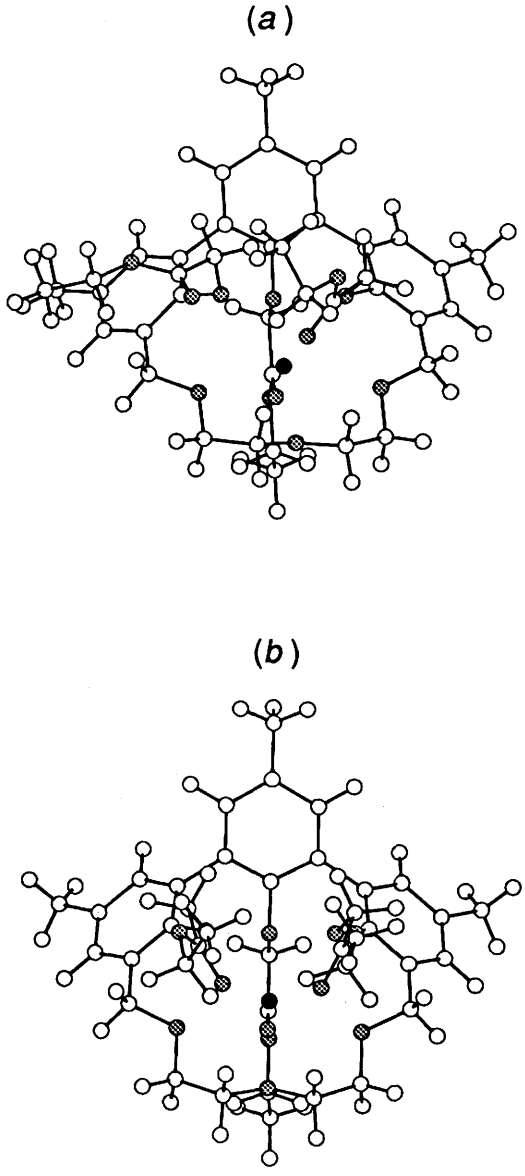

Fig. 4 Minimized structure (*a*) *in vacuo* and (*b*) structure of the calculated saddle points in the fast exchange process

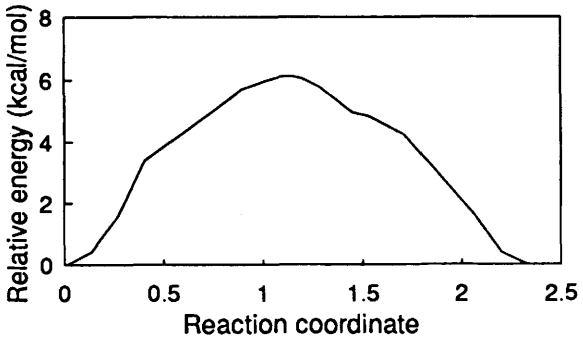

Fig. 5 Energy profile of fast exchange process

exchange process (kHz regime) of the two outer substituents, which leads to a time-averaged structure with a plane of symmetry. Simultaneous coordination of both outer carbonyl moieties cannot be the reason for the observed symmetry in solution because this structure can be regarded as the transition state in the fast exchange process.

Conclusions

Although the structures of **1**·$NaClO_4$ in the solid state and in methanol solution are very similar, the dynamics are very different. In solution a fast interconversion of conformations in which either one of the outer carbonyl groups is coordinated to the Na^+ occurs, with both outer carbonyl groups coordinated to the Na^+ in the transition state. The overall structure in solution is similar to the solid-state structure. The computational results are fully in line with the experimental observations and show that the Conjugate Peak Refinement module is a powerful tool with which to calculate true saddle points.

Experimental

X-Ray structure determination

The cell parameters were obtained by least-squares fit using 25 centred reflections with $6 < \theta < 25°$ (Table 2). An Enraf-Nonius CAD-4 diffractometer was used for data collection, 5119 unique reflections for $0 \leqslant h \leqslant 20$, $0 \leqslant k \leqslant 22$ and $0 \leqslant l \leqslant 24$. Intensities were measured in the $\omega/2\theta$ scan mode [scan speed 0.0915 deg s^{-1}, scan width (0.9 + 0.35) tan θ]. Decay of three control reflections, measured every hour, was < 1%. Correction was made for Lorentz and polarization factors. The number of observed reflections was 2525 [$F_o^2 > 3\sigma(F_o^2)$]. Absorption correction was made with DIFABS. The structure was solved by direct methods and refined by full-matrix least squares. The weight for each reflection in the refinement (on F) was calculated from $w = 4F_o^2/\sigma^2(F_o^2)$, $\sigma^2(F_o^2) = \sigma^2(I) + (pF_o^2)^2$; the value of the instability factor p was determined as 0.05. Hydrogen atoms were placed in calculated positions and were refined. The number of parameters refined was 552: scale factor, isotropic extinction factor g [$F_{corr} = Fc/(1 + gIc)$; final value 9.4×10^{-8}], positional and anisotropic thermal parameters for all non-hydrogen atoms and positional and isotropic thermal parameters for all hydrogens. Refinement converged at $R = 4.87\%$ and $R_w = 5.26\%$. All calculations were performed with the SDP package.[25] Atomic scattering factors were taken from ref. 26. Atomic coordinates and thermal parameters have been deposited at the Cambridge Crystallographic Data Centre.¶

Synthesis

$1^5,2^5,3^5$-Trimethyl-$1^2,2^2,3^2$-tris(prop-2-en-1-yloxy)-5,8,11-trioxa-1,2,3(1,3)-tribenzenacyclododecaphane–$NaClO_4$, 4·$NaClO_4$. A solution of 3,3″-bis(bromomethyl)-5,5′,5″-trimethyl-2,2′,2″-tris(prop-2-en-1-yloxy)-1,1′:3′,1″-terphenyl **3** (5.38 g, 8.59 mmol) and diethylene glycol (0.91 g, 8.59 mmol) in 100 cm^3 tetrahydrofuran (THF) was added to a refluxing suspension of 4 mol equiv. of NaH (0.83 g) in 400 cm^3 THF over a period of 10 h. The reaction was performed under a dry nitrogen atmosphere. After the addition was completed the reaction mixture was refluxed for an additional 3 h after which it was cooled to room temperature. Subsequently 10 cm^3 of water were carefully added to destroy the remaining NaH. After evaporation of the THF the residue was dissolved in a mixture of MeOH and CH_2Cl_2 (100 cm^3; 1:1) and a solution of 1 mol equiv. $NaClO_4 \cdot H_2O$ in 10 cm^3 MeOH was added. This mixture was concentrated to *ca.* 40 cm^3 after which an off-white precipitate was obtained. It was filtered off and washed once with MeOH to give a 64% yield of 4·$NaClO_4$.

Mp 147 °C. $\delta_H(CDCl_3)$ 7.30 (2 H, s, ArH^i), || 7.10 (2 H, d, J 2.0 Ar H°),|| 7.04 (2 H, d, J 2.0, ArH°), 5.86–5.73 (2 H, m, CH=°), 5.03–4.84 (5 H, m, $CH^{=i}$ and CH_2=°), 4.92 and 4.00 (4 H, AB, J 9.0, $ArCH_2O$), 4.77–4.37 and 4.53–4.43 (2 H, m, H, $=CH_2^i$),

¶ For details of the CCDC deposition scheme, see 'Instructions for Authors (1996)', *J. Chem. Soc., Perkin Trans. 2*, 1996, Issue 1.

||Here and elsewhere ^{i} refers to inner groups and ^{o} refers to outer groups.

Table 2 Data collection and crystal parameters for **1**·$NaClO_4$

Formula	$C_{39}H_{48}ClNaO_{16}$
f_w	831.25
Lattice type	Orthorhombic
Space group	P_{212121}
T/K	293
Cell dimensions	
a/Å	14.665(2)
b/Å	15.975(2)
c/Å	17.327(2)
V/Å^3	4059(2)
Z	4
D_c/g cm^{-3}	1.36
$F(000)$	1752
μ/cm^{-1}	1.71
θ Range/degrees	3–27.5
Data collected	
No. of unique reflections measured	5119
No. of reflections observed [$I > 3\sigma(I)$]	2525
No. of variables	552
R (%)	4.87
R_w (%)	5.26
Weighting factor p	0.05
Extinction g	9.4×10^{-8}
$\lambda_{radiation}$ (Mo-Kα)/Å	0.7107

4.53–4.43 and 4.30–4.23 (4 H, m, OCH_2), 4.07–3.99 and 3.58–3.44 (8 H m, $ArOCH_2°$ and OCH_2), 2.90–2.86 (2 H, m, $ArOCH_2^i$), 2.52 (3 H, s, $ArCH_3^i$) and 2.34 (6 H, s, $ArCH_3°$). $\delta_C(CDCl_3)$** 153.5 (ArC–O°), 151.8 (ArC–O^i), 120.3 (=$CH_2°$), 120.1 (=CH_2^i), 76.1 ($ArOCH_2°$), 74.8 ($ArOCH_2^i$), 71.8, 70.7 and 69.5 (OCH_2), 21.1 ($ArCH_3^i$) and 20.9 ($ArCH_3°$). FABMS (NBA), m/z 593 ($[M + Na]^+$).

$1^2,2^2,3^2$-Trihydroxy-$1^5,2^5,3^5$-trimethyl-5,8,11-trioxa-1,2,3(1,3)-tribenzenacyclododecaphane, 5. A mixture of **4**·$NaClO_4$ (3.82 g. 3.98 mmol), 5 mol% $Pd(OAc)_2$, 20 mol% Ph_3P, 3 mol equiv. of Et_3N and 3 mol equiv. of HCOOH in 100 cm^3 EtOH and 20 cm^3 water was refluxed for 1 h. The resulting mixture was cooled to 5 °C to give **5** as a precipitate. It was filtered off and dried in a vacuum oven at 80 °C. The crude product (90%) was pure on the NMR scale and was used without further treatment.

Mp 196 °C. $\delta_H([^2H_6]DMSO)$ 7.15 (2 H, s, Ar H^i), 7.08 (2 H, d, J 2.0, ArH°), 6.88 (2 H, d, J 2, ArH°), 4.58 (4 H, bs, $ArCH_2$), 3.68–3.60 (4 H, m, OCH_2), 3.57–3.50 (4 H, m, OCH_2), 2.36 (3 H, s, $ArOCH_3^i$), 2.26 (6 H, s, $ArCH_3°$). $\delta_C([^2H_6]DMSO)$** 151.6 (Ar C–O°), 149.9 (Ar C–O^i), 71.0, 70.5 and 68.8 (OCH_2), 20.8 ($ArCH_3^i$) and 20.4 ($ArCH_3°$). ν_{max}(KBr)/cm^{-1} 3414 (OH). EI-MS, m/z 450 (M^+).

$1^2,2^2,3^2$-Tris(ethoxycarbonylmethoxy)-$1^5,2^5,3^5$-trimethyl-5,8,11-trioxa-1,2,3(1,3)-tribenzenacyclododecaphane, hemispherand 1·$NaClO_4$. A mixture of **5** (1.00 g, 2.22 mmol), ethyl bromoacetate (4 mol equiv.) and K_2CO_3 (4 mol equiv.) was refluxed in 50 cm^3 acetonitrile for 1.5 h after which it was cooled to room temperature. The salts were filtered off and washed once with acetonitrile. The combined organic layers were concentrated and the residue was dissolved in 10 cm^3 MeOH. After the addition of 1 mol equiv. of $NaClO_4$·H_2O the solution was concentrated to *ca.* 3 cm^3 to give **1**·$NaClO_4$ as an off-white precipitate. It was filtered off and washed once to give the complex in 63% yield.

Mp 233 °C. $\delta_H(CD_3OD)$ 7.47 (2 H, s, ArH^i), 7.25 (2 H, d, J 2.0, ArH°), 7.18 (2 H, d, J 2.0, ArH°), 5.01 and 4.22 (4 H, AB, J 10.0, $ArCH_2$), 4.22–4.07 (4 H, ABX_3, $OCH_2CH_3°$), 4.22 and 4.04 (4 H, AB, J 16.0, $ArCH_2O°$), 3.97 (2 H, q, J 7.0, $OCH_2CH_3^i$), 4.0–3.9 (2 H, m, OCH_2), 3.9–3.8 (2 H, m, OCH_2), 3.7–3.6 (4 H, m, OCH_2), 3.10 (2 H, s, $ArOCH_2^i$), 2.54 (3 H, s, $ArCH_3^i$), 2.38 (6 H, s, $ArCH_3°$), 1.25 (6 H, t, J 7.0, $OCH_2CH_3°$) and 1.05 (3 H, t, J 7.0, $OCH_2CH_3^i$). $\delta_C(CD_3OD, 303\ K)$** 171.2 (C=O°), 170.2 (C=O^i), 155.6 (Ar C–O°), 150.1 (Ar C–O^i), 138.3 (ArC–Me^i), 136.5 (Ar C–Me°), 72.4 (CH_2O), 72.1 (OCH_2), 71.8 ($ArCH_2$), 71.5 ($ArOCH_2°$), 69.2 ($ArOCH_2^i$), 62.8 ($OCH_2CH_3°$), 62.5 ($OCH_2CH_3^i$), 21.3 ($ArCH_3^i$), 20.8 ($ArCH_3°$), 14.4 ($OCH_2CH_3°$) and 14.2 ($OCH_2CH_3^i$). FABMS (NBA), m/z 731 ($[M + Na]^+$) (Found: C, 55.4, H, 6.0. Calc. for $C_{39}H_{48}ClNaO_{16}$·H_2O: C, 55.16; H, 5.93%).

** Only 'informative' peaks are given.

NMR studies

Measurements were preformed at 400 MHz on a Varian Unity 400 WB spectrometer (J values are given in Hz). NOESY, ROESY, DQF-COSY (double-quantum filtered correlation spectroscopy), TQ-COSY (triple-quantum filtered correlation spectroscopy) and HMQC (heteronuclear multiple quantum spectroscopy) experiments were performed using standard Varian pulse programs. The mixing of the NOESY experiments ranged from 50 to 300 ms. $T_{1\rho}$ measurements were performed using the pulse-sequence $(\pi/2) - \tau_{spinlock}$ with phase alternation of the $\pi/2$ pulse. The CPMAS experiment was performed using a 5 mm SiN_3 rotor spinning at 7 kHz. A high power proton decoupling field of *ca.* $\gamma B_1/2\pi = 55$ kHz was used. Upon establishment of the Hartman–Hahn condition a contact-time of 2 ms was used. The relaxation delay was set to 7 s. All 2D experiments were collected as hypercomplex data. Data were Fourier transformed in the phase-sensitive mode using after weighting with shifted square sine-bells or shifted Gaussian functions. NMR data were processed by the standard Varian VNMRS/- VNMRX software installed on a SUN Sparc 10 computer.

Computational methods

The coordinates from the X-ray structure were used as the starting point. Additional required input files as well as visualizations were done with Quanta 3.3.[27] Minimizations were carried out with CHARMm 22.0,[20] as implemented in the Quanta/CHARMm package. Saddle point calculations were run with CHARMm 22g3.[20] Parameters were taken from Quanta 3.3 and point charges were calculated with the charge template option in Quanta.†† The ligand was charged to zero with a small 'excess' charge smoothed to non-polar carbons and hydrogens. The structures were minimized by ABNR (Adopted-Basis set Newton-Raphson) until the RMS of the energy gradient was < 0.001 kcal mol^{-1} Å^{-1}. No cut-off on the non-bonded interactions was applied. A distant dependent relative permittivity was chosen. Saddle point calculations were carried out with the Conjugate Peak Refinement (CPR) with an initial path-scanning step-size $\Delta\lambda$ of 0.05. This is the only parameter of the CPR method that has a system dependent optimum. It is automatically reduced until an optimum is reached. The output of CPR consists of a series of N intermediate structures along the reaction pathway including one or more saddle points. After the saddle point was fully refined by CPR the other points along the path were further relaxed into the adiabatic valleys of the energy by Steepest Descent Path, followed by Synchronous Chain Minimization.[21] The RMS of the gradient of the saddle point was 1.3×10^{-6} kcal mol^{-1} Å^{-1}. The MD simulation was performed as follows. A structure with the two outer carbonyl groups co-ordinated to the Na^+ was placed in the centre of a cubic box of OPLS MeOH[24] of 30.747 Å dimensions. Initially the box was filled with 429 molecules of MeOH and solvent molecules at a distance ≤2.3 Å, based on heavy atoms, with the Na^+ complex were deleted. Full periodic boundary conditions were used. The system was

†† The parameters are available as supplementary data (SUPP. No. 57118) from the British Library. For details of the Supplementary Publications Scheme see 'Instructions for Authors (1996)', *J. Chem. Soc., Perkin Trans. 2*, 1996, Issue 1.

minimized by steepest descent (200 steps) and Powell until the RMS of the energy gradient was $\leqslant 0.01$ kcal mol^{-1} $Å^{-1}$ or a maximum of 2000 steps was reached. NOE constraints were applied to the two $C{=}O_{outer} \cdots Na^+$ distances (3.4–3.6 Å). The system was heated to 300 K in 5 ps. Scaling of velocities was attempted every 50 steps with a temperature window of 10 K. The production phase was 50 ps long in which no NOE constraints were imposed. The van der Waals interactions were treated with the switch function (truncated between 10 and 13 Å) and the electrostatic interaction with the shift function with a cut-off of 14 Å. A constant relative permittivity and an ε value of 1 were used. Coordinates were saved every 200 time steps. The SHAKE algorithm [28] was used on all bonds involving hydrogen atoms, allowing a time step of 1 fs.

Acknowledgements

We gratefully acknowledge Akzo Research Laboratories Arnhem, The Netherlands, for financial support.

References

1 W. F. van Straaten-Nijenhuis, F. de Jong and D. N. Reinhoudt, *Recl. Trav. Chim. Pays-Bas*, 1992, **112**, 317; W. F. van Straaten-Nijenhuis, F. de Jong, D. N. Reinhoudt, R. P. Thummel, T. W. Bell and J. Liu, *J. Membr. Sci.*, 1993, **82**, 277; H. C. Visser, D. N. Reinhoudt and F. de Jong, *Chem. Soc. Rev.*, 1994, **23**, 75.

2 P. L. H. M. Cobben, R. J. M. Egberink, J. G. Bomer, R. Schouwenaar, Z. Brzøzka, M. Bos, P. Bergveld and D. N. Reinhoudt, *Anal. Chim. Acta*, 1993, **276**, 347; D. N. Reinhoudt and P. L. H. M. Cobben, *Dechema-Monographien Band 126*, VCH, Weinheim, 1992, pp. 219; P. L. H. M. Cobben, R. J. M. Egberink, J. G. Bomer, P. Bergveld, W. Verboom and D. N. Reinhoudt, *J. Am. Chem. Soc.*, 1992, **114**, 10 573.

3 J.-D. van Loon, J. F. Heida, W. Verboom and D. N. Reinhoudt, *Recl. Trav. Chim. Pays-Bas*, 1992, **111**, 353; L. C. Groenen and D. N. Reinhoudt, *Supramolecular Chemistry*, eds. V. Balzani and L. De Cola, Kluwer, Dordrecht, 1992, 51.

4 J. A. J. Brunink, R. J. W. Lugtenberg, Z. Brzøzka, J. F. J. Engbersen and D. N. Reinhoudt, *J. Electroanal. Chem.*, 1994, **378**, 185; J. A. J. Brunink, J. G. Bomer, J. F. J. Engbersen, W. Verboom and D. N. Reinhoudt, *Sensors and Actuators B*, 1993, **15–16**, 195; J. A. J. Brunink, W. Verboom, J. F. J. Engbersen, S. Harkema and D. N. Reinhoudt, *Recl. Trav. Chim. Pays-Bas*, 1992, **111**, 511.

5 P. D. van der Wal, E. J. R. Sudhölter and D. N. Reinhoudt, *Anal. Chim. Acta*, 1991, **245**, 159.

6 D. J. Cram, *Science*, 1988, **240**, 760; J. K. Judice, S. J. Keipert, C. B. Knobler and D. J. Cram, *J. Chem. Soc., Chem. Commun.*, 1993, 1325 and references cited therein.

7 R. A. W. Johnstone and M. E. Rose, *J. Chem. Soc., Chem. Commun.*, 1983, 1268.

8 L. X. Dang and P. A. Kollman, *J. Am. Chem. Soc.*, 1990, **112**, 5716.

9 M. A. Thompson, E. D. Glendening and D. Feller, *J. Phys. Chem.*, 1994, **98**, 10 465.

10 Y. A. Ovchinnikov and V. T. Ivanov, *Tetrahedron*, 1974, **30**, 1871.

11 W. L. Duax, H. Hauptman, C. M. Weeks and D. A. Norton, *Science*, 1972, **176**, 911; J. L. Karle, *J. Am. Chem. Soc.*, 1975, **97**, 4379; G. D. Smit, W. L. Duax, D. A. Langs, G. T. de Titta, J. W. Edmonds, D. C. Rohrer and C. M. Weeks, *J. Am. Chem. Soc.*, 1975, **97**, 7242.

12 W. I. Iwema Bakker, M. Haas, C. Khoo-Beattie, R. Ostaszewksi, S. M. Franken, H. J. den Hertog Jr., W. Verboom, D. de Zeeuw, S. Harkema and D. N. Reinhoudt, *J. Am. Chem. Soc.*, 1994, **116**, 123.

13 Synthetic details will be published in a forthcoming paper.

14 T. Yamada, K. Goto, Y. Mitsuda and J. Tsuji, *Tetrahedron Lett.*, 1987, **28**, 4557.

15 P. J. Dijkstra, H. J. den Hertog, Jr., J. van Eerden, S. Harkema and D. N. Reinhoudt, *J. Org. Chem.*, 1988, **53**, 374.

16 M. F. Summers, L. G. Marzilli and A. Bax, *J. Am. Chem. Soc.*, 1986, **108**, 4285.

17 M. Rance, O. W. Sörensen, G. Bodenhausen, G. Wagner, R. R. Ernst and K. Wüthrich, *Biochem. Biophys. Res. Commun.*, 1983, **117**, 479.

18 U. Piantini, O. W. Sörensen and R. R. Ernst, *J. Am. Chem. Soc.*, 1982, **104**, 6800.

19 C. Deverell, R. E. Morgan and J. H. Strange, *Molecular Physics*, 1970, **18**, 553; K. D. Kopple, Y.-E. Wang, A. G. Chang and K. K. Bhandary, *J. Am. Chem. Soc.*, 1988, **110**, 4168.

20 B. R. Brooks, R. E. Bruccoleri, B. D. Olafsen, D. J. States, S. Swaminathan and M. Karplus, *J. Comput. Chem.*, 1983, **4**, 187; F. A. Momany and R. Rone, *J. Comput. Chem.*, 1992, **13**, 888.

21 S. Fischer and M. Karplus, *Chem. Phys. Lett.*, 1992, **194**, 252.

22 S. Fischer, P. D. J. Grootenhuis, L. C. Groenen, W. P. van Hoorn, F. C. J. M. van Veggel, D. N. Reinhoudt and M. Karplus, *J. Am. Chem. Soc.*, 1995, **117**, 1611.

23 P. Timmerman, W. Verboom, F. C. J. M. van Veggel, J. P. M. van Duynhoven and D. N. Reinhoudt, *Angew. Chem., Int. Ed. Engl.*, 1994, **33**, 2345.

24 W. L. Jorgensen, *J. Phys. Chem.*, 1986, **90**, 1276.

25 B. A. Frenz & Associates, Inc., SDP Structure Determination Package, College Station, Texas, USA, 1983.

26 International Tables for X-Ray Crystallography, vol. IV, The Kynoch Press, Birmingham, 1974, Table 2.2B.

27 Quanta was bought from Molecular Simulations Inc., Burlington, MA, USA.

28 H. J. C. Berendsen, J. P. M. Postma, A. di Noia, W. F. van Gunsteren and J. R. Haak, *J. Chem. Phys.*, 1984, **81**, 3684.

Paper 5/03223G
Received 22nd *May* 1995
Accepted 11*th September* 1995